

Tissue-Saving Zernike Terms Selection in Customized Treatments for Refractive Surgery

Samuel Arba-Mosquera^{1,2}, Diego de Ortueta³ and Jesús Merayo-Llodes¹

ABSTRACT

PURPOSE: To study the possibility of performing customized refractive surgery minimising the amount of ablated tissue without compromising visual quality.

METHODS: A new algorithm for the selection of an optimized set of Zernike terms in customized treatments for laser corneal refractive surgery was developed. Its tissue saving attributes have been simulated on 100 different wave aberrations at 6mm diameter. Outcomes were evaluated in terms of how much depth and volume was saved for each condition (in micrometers and in percentage), whether the proposed correction consists of either a full wavefront correction or an aberration-free treatment, and whether the proposed depth or volume was less than the one required for the equivalent aberration-free treatment.

RESULTS: Simulated outcomes showed an average saved depth of 5µm (0-16µm), and an average saved volume of 95µl (0-127µl) or 11% saved tissue (0-66% saved tissue). Proposed corrections were always less deep than full wavefront corrections and in 59% of the cases were less deep than equivalent aberration-free treatments.

CONCLUSIONS: Even though Zernike modes decomposition is a mathematical description of the aberration, it is not the aberration itself. Not all Zernike modes affect the optical quality in the same way. The eye does not see through Zernike decomposition but with its own aberration pattern. However, it seems feasible to efficiently perform laser corneal refractive surgery in a customized form minimising the amount of ablated tissue without compromising the visual quality. Further clinical evaluations on human eyes are needed to confirm the preliminary simulated results presented herein. (J Optom 2009;2:182-196 ©2009 Spanish Council of Optometry)

KEY WORDS: refractive surgery; visual quality; Zernike; tissue saving; wavefront; aberrations; depth; volume; time; aberration-free; free of aberrations; diffraction limited.

RESUMEN

OBJETIVO: Estudiar la posibilidad de realizar tratamientos personalizados de cirugía refractiva donde se minimice la cantidad de tejido ablacionado sin que por ello se vea afectada la calidad visual.

MÉTODOS: Se ha desarrollado un nuevo algoritmo para seleccionar un conjunto optimizado de términos de Zernike para su aplica-

ción en tratamientos personalizados de cirugía refractiva corneal. Para 100 mapas de aberración de onda corneal (para un tamaño de pupila de 6 mm de diámetro), se ha simulado la capacidad de dicho algoritmo para preservar tejido corneal. El resultado de dicha simulación se ha analizado en función de cuanto espesor (en micras) o de cuanto volumen (en %) se preserva en cada situación (respecto a otra situación de referencia): si la corrección propuesta logra corregir todo el frente de onda o sólo las aberraciones de segundo orden, y si el espesor o el volumen que hay que ablacionar con esta configuración es menor que para un tratamiento estándar equivalente, donde se traten de corregir únicamente las aberraciones de segundo orden.

RESULTADOS: Las simulaciones arrojaron un "ahorro" promedio de tejido ablacionado igual a 5 µm en términos de espesor máximo que se ha de ablacionar (rango: 0-16 µm), igual a 95 µl en términos de volumen (rango: 0-127 µl); esto es, se preserva un 11% del tejido (rango: 0-66%) respecto al tratamiento de referencia. Las correcciones propuestas siempre requerían espesores ablacionados menores que los patrones diseñados para corregir todo el frente de onda, y en el 59% de los casos requerían incluso un espesor menor que los tratamientos estándar (aquellos en los que se pretende corregir únicamente las aberraciones de segundo orden).

CONCLUSIONES: A pesar de que la descomposición en modos de Zernike es una descripción matemática de un patrón de aberración dado, no se corresponde exactamente con dicha aberración. No todos los modos de Zernike tienen el mismo efecto sobre la calidad óptica. El ojo no percibe su entorno "a través de" una descomposición en modos de Zernike de la aberración de onda, sino que se ve afectado por todo su propio patrón de aberración, de manera conjunta. Sin embargo, parece factible el llevar a cabo de manera eficiente tratamientos personalizados de cirugía refractiva corneal donde se minimice la cantidad de tejido ablacionado sin que por ello se vea afectada la calidad visual.

Es necesario hacer más estudios en ojos humanos reales para poder confirmar los resultados preliminares de las simulaciones que aquí se presentan.

(J Optom 2009;2:182-196 ©2009 Consejo General de Colegios de Ópticos-Optometristas de España)

PALABRAS CLAVE: cirugía refractiva; calidad visual; Zernike; preservación de tejido; frente de onda, aberraciones; espesor; volumen; tiempo; sin aberraciones (de segundo orden); libre de aberraciones (de segundo orden); limitado por difracción.

From the ¹Instituto de Oftalmobiología Aplicada, University of Valladolid, Spain. ²Schwind eye-tech-solutions, Kleinostheim, Germany. ³Augenzentrum Recklinghausen, Recklinghausen, Germany.

Acknowledgements: This paper is part of the Arba-Mosquera's doctoral thesis project at the Instituto Universitario de Oftalmobiología Aplicada (IOBA) in partial fulfilment of the requirements for the academic degree of Doctor of Philosophy (PhD) in Sciences of Vision, Research Group "Cirugía Refractiva y Calidad de Visión".

Received: 12 January 2009

Revised: 4 June 2009

Accepted: 25 June 2009

Corresponding author: Samuel Arba Mosquera.
Schwind eye-tech-solutions
e-mail: samuel.arba.mosquera@eye-tech.net

INTRODUCTION

With the introduction of laser technology for refractive surgery, the procedure of changing the curvature of the cornea in a controlled manner¹ to compensate for refractive errors of the eye is nowadays more accurate than ever. However, the quality of vision still deteriorates significantly, especially under mesopic and low-contrast conditions.²

With the LASIK (laser in-situ keratomileusis)³ treatment, we have an accepted method for correcting refractive errors such as myopia,⁴ hyperopia,⁵ and astigmatism.⁶ One of the

most significant side effects in myopic LASIK is the induction of spherical aberration,⁷ which causes halos, and a reduction of contrast sensitivity.²

Although the optical quality of the eye can be described in terms of the aberration of its wavefront, it was observed that the subjects with minor aberrations in their wavefront did not always achieve the best scores in visual-quality tests.⁸ Thus, the optical quality of the human eye does not determine in a one-to-one way its visual quality.

However, the induction of aberrations, such as spherical aberrations and coma, has been related to a loss of visual acuity.⁹ Finally, the concept of neural compensation suggests that the neural visual system is adapted to the eye's own aberration pattern. A study by Artal et al.¹⁰ on the effects that this neural compensation causes on the visual function indicates that the visual quality we have is somewhat superior to the optical quality that our eye provides.

To avoid inducing aberrations, as well as to eliminate the existing aberrations, "customized" treatments were developed. Customization of the ablation procedure is possible, either using wavefront measurements of the whole eye¹¹ (obtained, e.g., by means of Hartman-Shack wavefront sensors) or by using corneal topography-derived wavefront analyses.^{12,13} Topography-guided,¹⁴ wavefront-guided,¹⁵ wavefront-optimized,¹⁶ asphericity-preserving, and Q-factor profiles¹⁷ have all been put forward as solutions. Considerations such as the duration of the treatment, removal¹⁸ and remodelling of tissue, and, in general, the overall surgical outcome have made it difficult to establish a universal optimum profile. These considerations are interrelated in a multifactorial way, and may lead to clinical problems as corneal dehydration, ectasia or regression.

The development of new algorithms or ablation strategies for performing laser corneal refractive surgery in a customized form minimising the amount of ablated tissue without compromising the visual quality becomes an important challenge.

The availability of such profiles, potentially maximising visual performance without increasing the risk factors, would be of great value for the refractive surgery community and, ultimately, for the patients' health and safety. Therefore, the topic "Optimized Zernike Term Selection in customized treatments for laser corneal refractive surgery" (OZTS) is worth to be analysed, because its clinical implications are not yet deeply explored.

The real impact of tissue-saving algorithms in customized treatments is still discussed in a controversial way. The problem of minimising the amount of tissue that is removed is that it must be done in such a way that: a) does not compromise the refractive correction; b) does not compromise visual performance; c) is safe, reliable and reproducible.

The goal of this study is to describe in detail the theoretical framework, explaining a possible method of tissue-saving optimisation and exploring its tissue-saving capabilities.

PATIENTS AND MATERIALS

To simulate the tissue-saving capabilities of such methods for minimising the required amount of ablated tissue, the

complete records (together with their clinical data) corresponding to one-hundred eyes of fifty-five patients (39 (71%) male and 16 (29%) female) from the Augenzentrum Recklinghausen (Germany) were selected to be included in our simulation experiment. Fifty-five were right eyes (55%), and forty-five were left eyes (45%).

The mean age was 32±8 years (ranging from 19 to 54). The spherical equivalent (SE) was 1.60 D with a standard deviation (SD) of 3.44 D (range -9.75 to +7.50 D), with a mean sphere of -0.85±3.08 D (SD) (range 8.25 to +7.50 D), the mean cylinder was 1.51±1.42 D (SD) (range 5.75 to 0.00 D).

Using the Keratron-Scout videokeratoscope¹⁹ (Optikon 2000, Rome, Italy), corneal wave aberrations were analysed up to the 7th Zernike order. Optical errors are described by means of the weight coefficients of the Zernike polynomials,²⁰ following the standards of the Optical society of America (OSA).²¹

For the purpose of the present work, SciLabTM was used for performing calculations and running the simulations, MicrosoftTM Excel for plotting graphs, and Delphi's programming language was used for implementing the modules in the Optimized Refractive Keratectomy (ORK) and the Custom Ablation Manager (CAM). To simulate the tissue-saving capabilities of such algorithms for minimising the required amount of ablated tissue, the CAM module with a newly implemented Optimized Zernike Terms Selection (OZTS) was used.

METHODS

In our study, the quadratic equivalent of a wave-aberration map was used as a relationship between wavefront-error magnitudes and classical ametropias (*Appendix 1*). That quadratic is a spherocylindrical surface, which approximates the wave aberration map. The idea of approximating an arbitrary surface with a quadratic equivalent is a simple extension of the ophthalmic technique of approximating a spherocylindrical surface with an equivalent sphere.

For this study, a variation of the objective wavefront refraction from low-order Zernike modes at a fixed subpupil diameter of 4 mm was chosen as starting point to objectively include the measured subjective manifest refraction in the wave aberration (*Appendix 2*).

The expected optical impact of high-order aberrations in the refraction is calculated and modified from the input manifest refraction. The same wave aberration is analysed for two different diameters: for the full wavefront area (6 mm in this study) and for a fixed subpupil diameter of 4 mm. The difference in refraction obtained for each of the two diameters corresponds to the manifest refraction associated to the high-order aberrations.

The condition is to re-obtain the input manifest refraction for the subpupil diameter of 4 mm. This way, the low-order parabolic terms of the modified wave aberration for the full wavefront area can be determined. An explanation of this Automatic Refraction Balance concept is provided in *figure 1*.

Figures 2 and *3* show examples of how the automatic manifest refraction balance algorithm works.

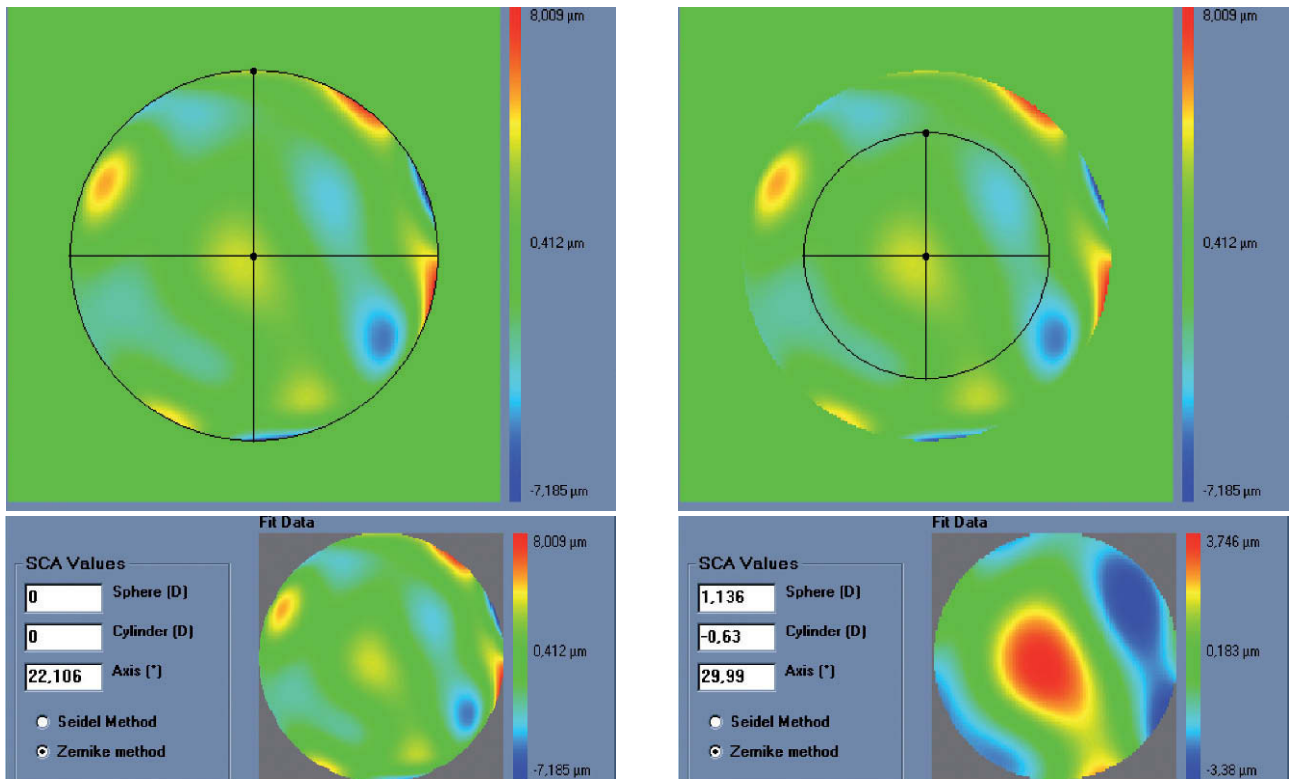


FIGURE 1 Automatic Refraction Balance. Optical impact of the HOA the refraction is calculated and balanced from input refraction. Notice that the same wave aberration is analysed for two different pupil diameters. The difference in the resulting refraction for these two diameters correspond to the manifest refraction associated to high-order aberrations.

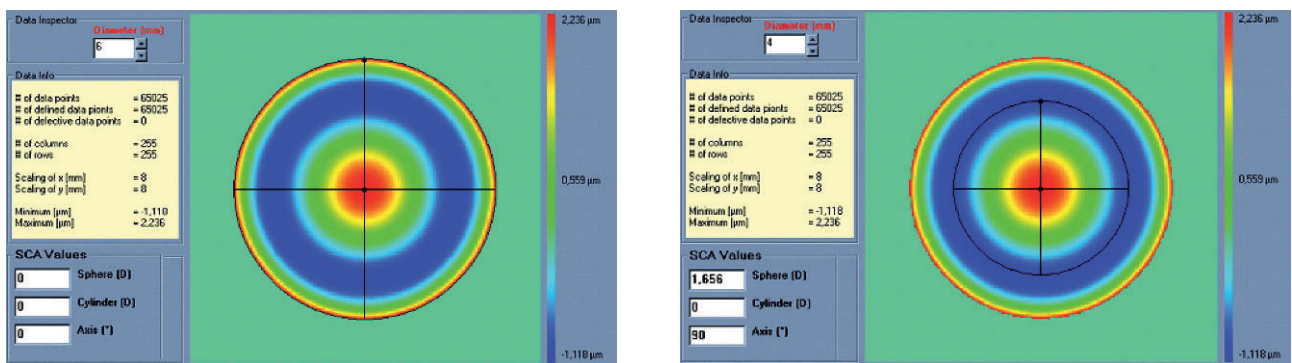


FIGURE 2 Left: Zernike refraction, for a 6 mm pupil size, of pure spherical aberration (SA). This refraction is per definition equal to 0 because SA is a high-order aberration mode. Right: Zernike refraction of the same wave aberration when analysed for a smaller pupil diameter (4 mm): SA (a high-order aberrations), when analysed for a smaller diameter, produces defocus. Explanation why a high-order aberration influences the low orders (refraction) when analysed for smaller diameters: for a full pupil (6 mm) the eye is affected by a SA producing some multifocality but without defocus; for a smaller pupil (4 mm), the optical aberration of the eye is the same but the outer ring is blocked. Thereby, the eye sees the world through the central part of a SA that resembles, in this case, a hyperopic profile producing some defocus (low-order refraction).

Objective Determination of the Actual Clinical Relevance of Each Separate Term in the Zernike Expansion of the Wave Aberration

A simple approach for the classification of the clinical relevance of individual aberration terms was proposed by Thibos et al.,²² by introducing the concept of equivalent

defocus (DEQ) as a metric to minimise the differences in the Zernike coefficients due to different pupil sizes.

Equivalent defocus is defined as the amount of defocus required to produce the same wavefront variance as found in one or more higher-order aberrations. A simple formula allows us to compute the equivalent defocus in dioptres if we

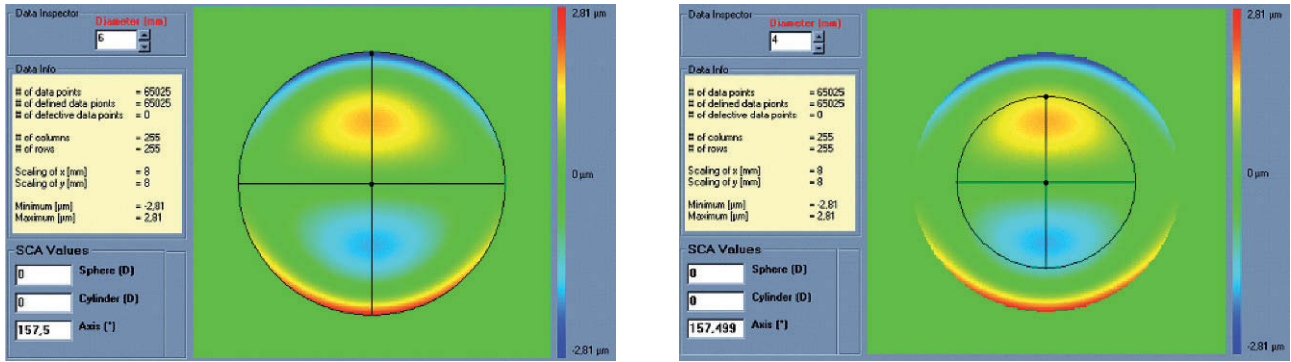


FIGURE 3
 Left: Zernike refraction of pure coma (for a 6 mm pupil), which is per definition equal to 0 because coma is a high-order aberration mode. Right: Zernike refraction of the same wave aberration when analysed for a smaller pupil diameter (4 mm). Pure coma (a high-order aberration), when analysed for a smaller pupil diameter, produces only high-order coma. Notice that coma may have a “visual effect” if the visual axis changes, resulting in astigmatism.

know the total wavefront variance associated to the Zernike modes of interest:

$$M_e = \frac{16\sqrt{3}RMS}{PD^2} \quad (1)$$

One could apply this concept of equivalent defocus to each individual Zernike mode in order to compute its clinical relevance. Of course, we must keep in mind that the kind of optical blur produced by higher-order aberrations is not the same as the blur produced by defocus. Nevertheless, this concept of equivalent defocus is helpful when it comes to interpreting the Zernike coefficients in familiar dioptric terms. The basis of the equivalent defocus concept is the notion that the imaging quality of an eye is determined primarily by wavefront variance, and that it does not matter which Zernike mode produces that variance. It is important to bear in mind that 1 dioptre of ordinary defocus does not necessarily have the same effect as 1 dioptre of equivalent defocus because different types of aberrations affect the retinal image in different ways.

Figure 4 depicts the effects on vision produced by 1 dioptre of equivalent defocus for each of the different Zernike terms, up to 7th order.

In general, for the same amount of equivalent defocus, the optical blur produced by higher-order aberrations increases with increasing radial order and decreases with increasing angular frequencies. Based on this blur effect of the individual Zernike terms we have defined a dioptric equivalent (DEq) of the form:

$$DEq_n^m = \frac{8\sqrt{2(n+1)(1+\delta_{m0})} |C_n^m|}{PD^2} \quad (2)$$

where DEq[n,m] is the optical blur for the individual Zernike term, n is the radial order of the Zernike term, m the meridional frequency of the Zernike term, δ_{m0} a delta function, PD the analysis diameter, and C[n,m] the weight coefficient of the Zernike term.

The relative optical blur of the Zernike polynomials up to 7th order is shown in table 1.

This dioptric equivalent metric is identical to the power vector notation for the low orders, and makes it possible to define a general optical blur of the form:

$$U_G = \sqrt{\sum DEq_q[n,m]} \quad (3)$$

as a generalization of the expression proposed by Thibos et al.²³

Using common clinician limits, the following classification is proposed:

Not clinically relevant $DEq_n^m \leq 0.25D$

Might be clinically relevant $0.25D < DEq_n^m \leq 0.50D$

Clinically relevant $DEq_n^m > 0.50D$

Objective Minimisation of the Maximum Depth of a Customized Ablation Based on the Zernike Expansion of the Wave Aberration

One of the minimisation approaches proposed in this work consists of simplifying the profile by selecting the subset of Zernike terms that minimises the necessary ablation depth while respecting the Zernike terms considered to be clinically relevant.

The “minimise depth”/“minimise depth+” function analyses the Zernike pyramid described in the previous section and evaluates the resulting ablation depth for all those possible free combinations of Zernike terms that fulfil the following conditions:

- Only 3rd- or higher-order terms can be disabled (excluded).
- Only those terms whose optical blur dioptric equivalent is less than 0.25 D can be disabled (0.50 D for “minimise depth+”)



FIGURE 4 Zernike pyramid showing the effects on vision produced by 1 dioptre of equivalent defocus of each individual Zernike term, up to 7th order.

–For each subset of Zernike terms, the low-order terms are recalculated using the Automatic Refraction Balance method described above

From this evaluation, the function selects the subset of Zernike terms for which the maximum ablation depth is minimal (*Appendix 3*).

Figure 5 shows an example of the “minimise depth +” function. Notice that 8 μ m of tissue are saved (16% of the

ablation depth), but that the overall shape of the ablation remains.

Objective Minimisation of the Ablation Volume of a Customized Ablation Based on the Zernike Expansion of the Wave Aberration

The other minimisation approach proposed in this work consists of simplifying the profile by selecting the subset of

TABLE 1
Relative optical blur of the Zernike polynomials up to 7th order (*continued*)

j = index	n = order	m = Frequency	Relative Optical Blur (Defocus = 1)
6	3	-3	$\sqrt{\frac{2}{3}} = 0.816$
7	3	-1	$\sqrt{\frac{2}{3}} = 0.816$
8	3	1	$\sqrt{\frac{2}{3}} = 0.816$
9	3	3	$\sqrt{\frac{2}{3}} = 0.816$
10	4	-4	$\sqrt{\frac{5}{6}} = 0.913$
11	4	-2	$\sqrt{\frac{5}{6}} = 0.913$
12	4	0	$\sqrt{\frac{5}{3}} = 1.291$
13	4	2	$\sqrt{\frac{5}{6}} = 0.913$
14	4	4	$\sqrt{\frac{5}{6}} = 0.913$
15	5	-5	1
16	5	-3	1
17	5	-1	1
18	5	1	1
19	5	3	1
20	5	5	1
21	6	-6	$\sqrt{\frac{7}{6}} = 1.080$
22	6	-4	$\sqrt{\frac{7}{6}} = 1.080$
23	6	-2	$\sqrt{\frac{7}{6}} = 1.080$
24	6	0	$\sqrt{\frac{7}{3}} = 1.528$
25	6	2	$\sqrt{\frac{7}{6}} = 1.080$ (.../...)

TABLE 1
Relative optical blur of the Zernike polynomials up to 7th order

j = index	n = order	m = Frequency	Relative Optical Blur (Defocus = 1)
26	6	4	$\sqrt{\frac{7}{6}} = 1.080$
27	6	6	$\sqrt{\frac{7}{6}} = 1.080$
28	7	-7	$\frac{2}{\sqrt{3}} = 1.155$
29	7	-5	$\frac{2}{\sqrt{3}} = 1.155$
30	7	-3	$\frac{2}{\sqrt{3}} = 1.155$
31	7	-1	$\frac{2}{\sqrt{3}} = 1.155$
32	7	1	$\frac{2}{\sqrt{3}} = 1.155$
33	7	3	$\frac{2}{\sqrt{3}} = 1.155$
34	7	5	$\frac{2}{\sqrt{3}} = 1.155$
35	7	7	$\frac{2}{\sqrt{3}} = 1.155$

Zernike terms that minimises the necessary ablation volume, while respecting those Zernike terms considered to be clinically relevant.

The “minimise volume”/“minimise volume+” function analyses the Zernike pyramid described in the previous section and evaluates the required ablation volume for all those possible free combinations of Zernike terms that fulfil the following conditions:

–Only 3rd- or higher-order terms can be disabled (excluded)

–Only those terms whose optical blur dioptric equivalent is below 0.25 D can be disabled (0.50 D for “minimise volume+”)

–For each combination (subset) of Zernike terms, the low-order terms are recalculated using the Automatic Refraction Balance method described above

From this evaluation, the function selects the subset of Zernike terms for which the required ablated volume is minimal (*Appendix 4*).

Figure 6 shows an example of the “minimise volume +” function.

A summary of the properties of the 4 minimisation approaches presented in this study are shown in *table 2*.

Simulation of the Tissue-saving Capabilities of These Methods for Minimising the Required amount of Ablated Tissue

For each wave aberration map, for a 6 mm pupil, it has been simulated how deep and how much volume of tissue was it necessary to ablate for 6 different scenarios:

- Correction of the full wavefront
- Minimising depth
- Minimising volume
- Minimising depth +
- Minimising volume +
- Equivalent aberration-free treatment

For each wave aberration, it has been calculated how much depth and volume of tissue was saved for each condition (in micrometers and in percentage, relative to the full wavefront correction), and it has been noted whether the proposed correction consists of either the full wavefront correction (with all Zernike terms included in the ablation) or the aberration-free treatment (without any Zernike term included in the ablation) and, finally, whether or not the proposed depth or volume was less than the one required for the equivalent aberration-free treatment.

Once the data about tissue saving was computed for each wave aberration, in order to calculate the average tis-

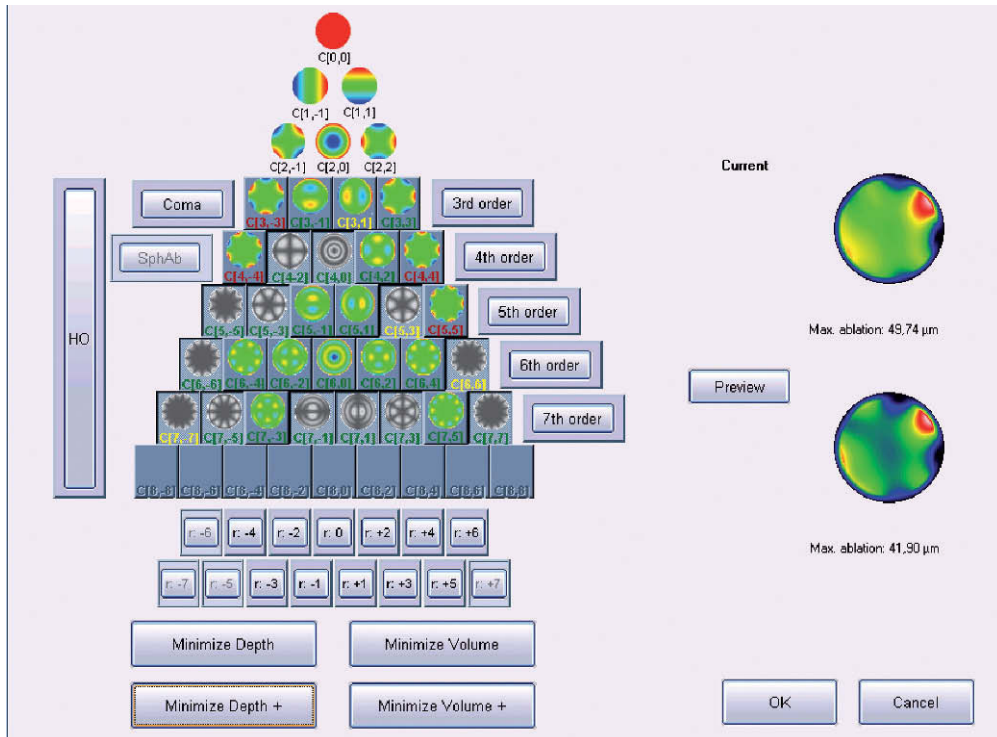


FIGURE 5 Objective analysis (Optimized Aberration-mode selection) of the optical and ablative effects of the different aberration modes for a given wavefront aberration (WFAb). Zernike terms that are considered not to be clinically relevant ($DEq \leq 0.25$ D) are marked in green, Zernike terms that might be considered to be clinically relevant (0.25 D < $DEq \leq 0.50$ D) are marked in yellow, and Zernike terms considered to be clinically relevant ($DEq > 0.50$ D) are marked in red. Note that the selection of aberration modes is not a trivial process: Not all the modes in green are unselected (not corrected) because some of them may help to save tissue. Not all aberration modes in yellow are selected (corrected) because some of them may have a low impact on vision. Notice, as well, that 8 μ m of tissue are saved (16% of the ablation depth), but that the overall shape of the ablation pattern hardly changes.

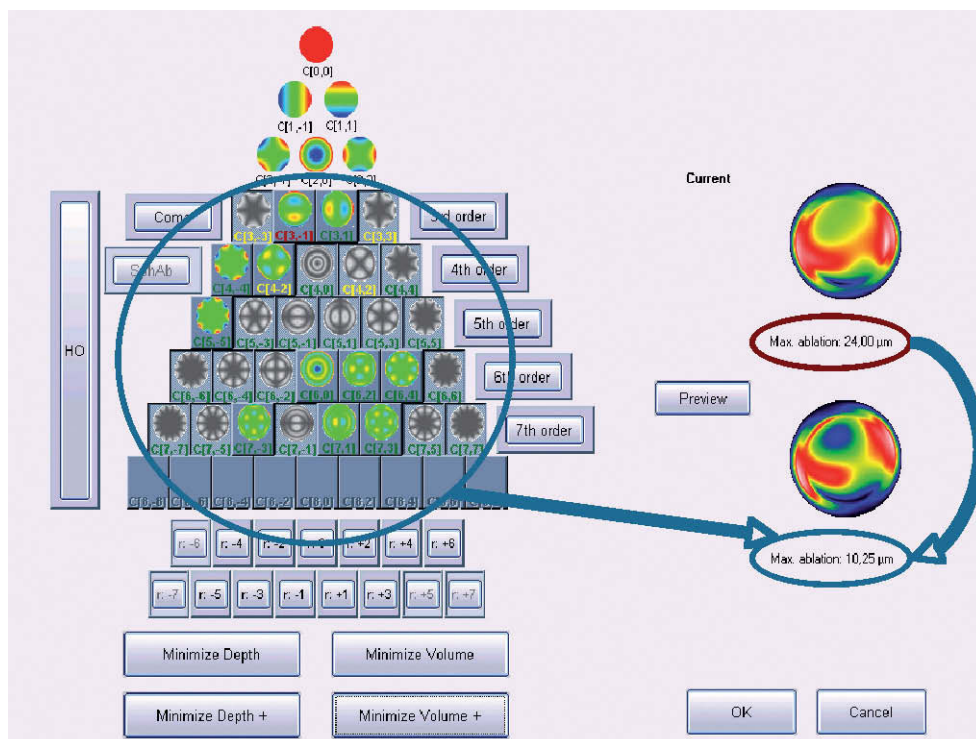


FIGURE 6 Optimized aberration-mode selection. Based on the wave aberration map, the software is able to recommend the best possible aberration-mode selection to minimise the amount of ablated tissue and time, without compromising the visual quality. Note that the wave aberration is analysed by the software showing the original ablation pattern required for a full wavefront correction and the suggested subset of aberration modes to be corrected. Notice the difference in terms of required ablated tissue, but notice as well that the most representative characteristics of the wavefront map are still present in the minimised-tissue selection.

TABLE 2
Summary properties of the 4 minimisation approaches

min Depth	min Depth +	min Vol	min Vol +
Only 3 rd -or higher-order terms (HOA terms) can be disabled			
Only terms with optical blur ≤ 0.25 D (green) can be disabled	Only terms with optical blur ≤ 0.50 D (green or yellow) can be disabled	Only terms with optical blur ≤ 0.25 D (green) can be disabled	Only terms with optical blur ≤ 0.50 D (green or yellow) can be disabled
For each subset of Zernike terms, Automatic Refraction Balance is used			
The subset of Zernike terms that results in the lowest value for the maximum depth is selected		The subset of Zernike terms that results in the minimum ablation volume is selected	

sue saving for the different modalities over the sample of treatments we have used several methods: a) direct average of the saved depth or volume; b) intercept with the axis in a correlation graph; c) direct average of the percentual saved depth or volume.

Statistical Analysis

Descriptive statistics: Determination of minimum, maximum, and mean values and of the corresponding simple standard deviation. The following statistics were employed: how much tissue is saved by means of this minimisation procedure and how often this procedure results in ablated depths or volume below the amount required for the aberration-free profile. For statistical analysis, *t*-tests were used, with *P* values below 0.05 being considered to be statistically significant.

RESULTS

Corneal Wave Aberration

The average root mean square for the high-order wave aberration (RMS_{HO}) was 0.555 ± 0.143 μm for a 6 mm pupil (range: from 0.327 to 0.891 μm), whereas the average root mean square of the total wave aberration (RMS) was 3.955 ± 2.715 μm also for a 6 mm pupil (range: from 0.741 to 10.920 μm).

The distribution of corneal aberration in its Zernike terms seems to be normal.

Spherical aberration was $+0.107 \pm 0.205$ μm (range: from -0.476 to +0.514 μm), coma aberration was 0.369 ± 0.316 μm (range: from 0.030 to 1.628 μm), and trefoil aberration was 0.204 ± 0.186 μm (range: from 0.022 to 1.118 μm); all of them refer to a 6 mm diameter zone.

Objective Determination of the Actual Clinical Relevance of Each Individual Term in the Zernike Expansion of the Wave Aberration

Spherical aberration was $+0.184 \pm 0.136$ DEq (range: from 0.000 to +0.511 DEq), coma aberration was 0.232 ± 0.199 DEq (range: from 0.019 to 1.023 DEq), and trefoil aberration was 0.128 ± 0.117 DEq (range: from 0.014 to 0.703 DEq).

Out of all the wave aberration maps under study, 72% of them showed a spherical aberration below 0.25 DEq, 23% of them showed a spherical aberration between 0.25 DEq and 0.50 DEq, and only 5% of the maps showed a spherical aberration higher than 0.50 DEq.

Regarding coma aberration, for 68% of the wave aberration maps it was below 0.25 DEq, for 23% of them it was between 0.25 DEq and 0.50 DEq, and only for 9% of the maps was the coma aberration higher than 0.50 DEq.

Regarding trefoil aberration, for 87% of the wave aberration maps it was below 0.25 DEq, for 10% of them it was between 0.25 DEq and 0.50 DEq, and only for 3% of the maps was the trefoil aberration higher than 0.50 DEq.

Simulation of the Tissue-Saving Capabilities of these Methods for Minimising the Required amount of Ablated Tissue

Comparing the ablations planned to correct for the whole wave aberration with equivalent aberration-free ablations (designed to correct only for spherocylindrical refraction), we observed an average difference in maximum depth of $+8 \pm 8$ μm (range: from -4 to +33 μm), and an average difference in volume of $+158 \pm 158$ μl (range: from -127 μl to +664 μl); that is, +32% (up to +317%), indicating that more tissue was necessary to ablate to achieve full customised corrections.

In 13% of the cases the ablations designed to correct for the whole wave aberration needed to ablate less tissue than the equivalent aberration-free ablations.

Comparing the proposed "minimised-depth" ablations with the equivalent ablations designed to correct for the whole wave aberration, we observed an average difference in maximum depth of -4 ± 2 μm (range: from -10 μm to -1 μm), and an average difference in ablated volume of -64 ± 32 μl (range: from -190 μl to 0 μl); that is, -8% (up to -30%), indicating that less tissue needs to be removed for the "minimised-depth" corrections.

In 43% of the cases, the proposed "minimised-depth" ablations resulted in less ablated tissue than the equivalent aberration-free ablations. Comparing the proposed "minimised-volume" ablations with the equivalent ablations devised

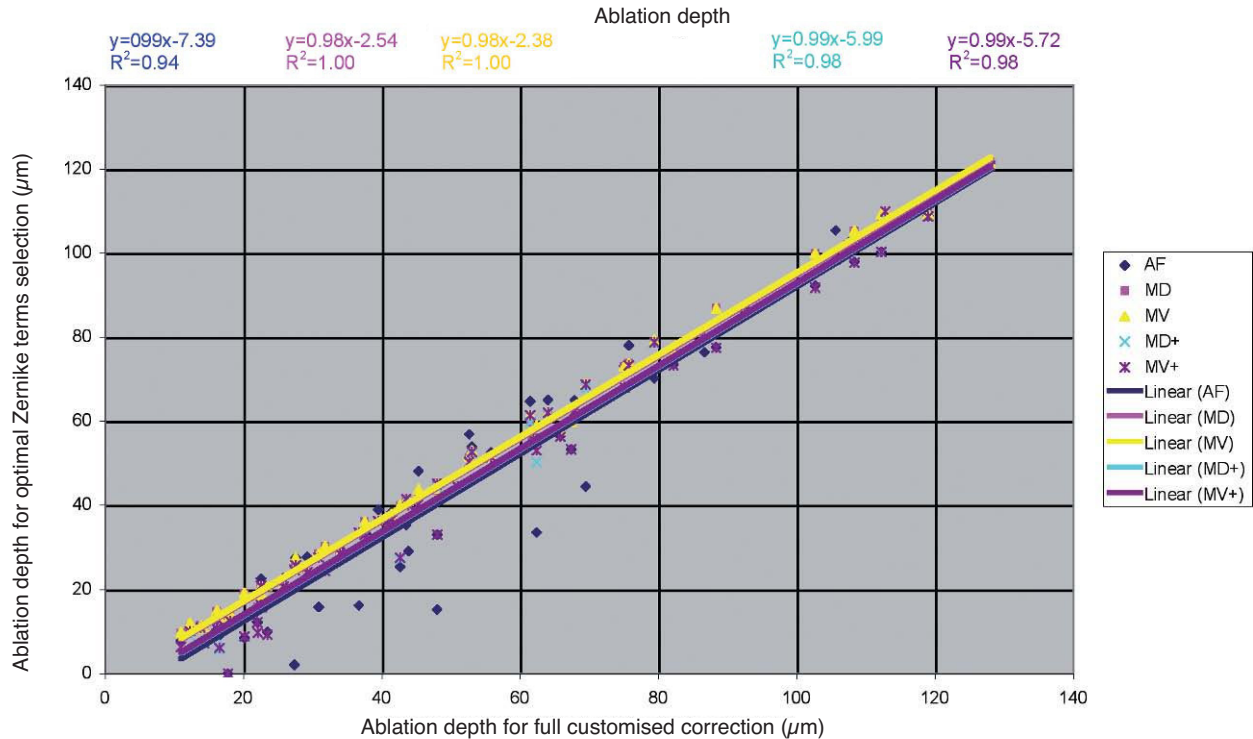


FIGURE 7

Ablation depth for the “Optimal Zernike Term Selection” method (OZTS) vs. Ablation depth for full customized correction, for the following modalities of OZTS: aberration-free correction (all HOA disabled) (AF, in blue), minimised depth (MD, in magenta), minimised volume (MV, in yellow), minimised depth+ (MD+, in cyan), and minimised volume+ (MV+, in purple).

to correct for the whole wave aberration, we observed an average difference in maximum depth of $-4 \pm 2 \mu\text{m}$ (range: from $-10 \mu\text{m}$ to $0 \mu\text{m}$), and an average difference in volume of $-64 \pm 32 \mu\text{l}$ (range: from $-190 \mu\text{l}$ to $0 \mu\text{l}$); that is -7% (up to -30%), meaning less tissue removal for the “minimised-volume” corrections.

In 39% of the cases, the proposed “minimised-volume” ablations required to remove less tissue than the equivalent aberration-free ablations (those devised to correct only for spherocylindrical refraction).

Comparing the proposed “minimised-depth+” ablations with the equivalent ablations designed to correct for the whole wave aberration, we observed an average difference in maximum depth of $-6 \pm 4 \mu\text{m}$ (range: from $-16 \mu\text{m}$ to $-1 \mu\text{m}$), and an average difference in volume of $-127 \pm 95 \mu\text{l}$ (range: from $-316 \mu\text{l}$ to $0 \mu\text{l}$) or -15% (up to -66%); that is, less tissue removal was required for the “minimised-depth+” corrections.

In 80% of the cases, the proposed “minimised-depth+” ablations needed less tissue than equivalent aberration-free ablations planned to correct only spherocylindrical refraction.

Comparing the proposed “minimised-volume+” ablations with the equivalent ablations intended to correct for the whole wave aberration, we observed an average difference in maximum depth of $-6 \pm 4 \mu\text{m}$ (range: from $-15 \mu\text{m}$ to $0 \mu\text{m}$), and an average difference in volume of $-127 \pm 64 \mu\text{l}$ (range: from $-316 \mu\text{l}$ to $0 \mu\text{l}$) or -14% (up to -63%); that is, less tissue removal was needed for the “minimised-volume+” corrections.

In 75% of the cases, the proposed “minimised-volume+” ablations needed to remove less tissue than the equivalent aberration-free ablations.

Detailed results comparing the different approaches can be found in *figure 7* for the ablation-depth-analysis and in *figure 8* for the ablation-volume-and-time analysis.

DISCUSSION

We have used the proposed dioptric equivalent applied to each individual Zernike mode in order to compute its clinical relevance. It is important to bear in mind that the orientation of the vector-like modes is not taken into account in our proposal, and 1 dioptre of cardinal astigmatism (at 0° , for example) doesn't necessarily have the same effect as 1 dioptre of oblique astigmatism (at 45° , for example). Despite this, other studies have proved this assumption to be reasonable.²⁴

One could use more sophisticated equations to model the equivalences between the optical blur produced by the different Zernike terms, but we have used a relatively simple approach driven primarily by the radial order.

Different approaches have been proposed for minimising tissue ablation in refractive surgery:

In multizonal treatments, the minimisation is based on the concept of progressively decreasing corrections in different optical zones. The problem comes from the aberrations that are induced (especially spherical aberration).

In the treatments designed having a smaller optical zone combined with bigger transition zones, the minimisation is

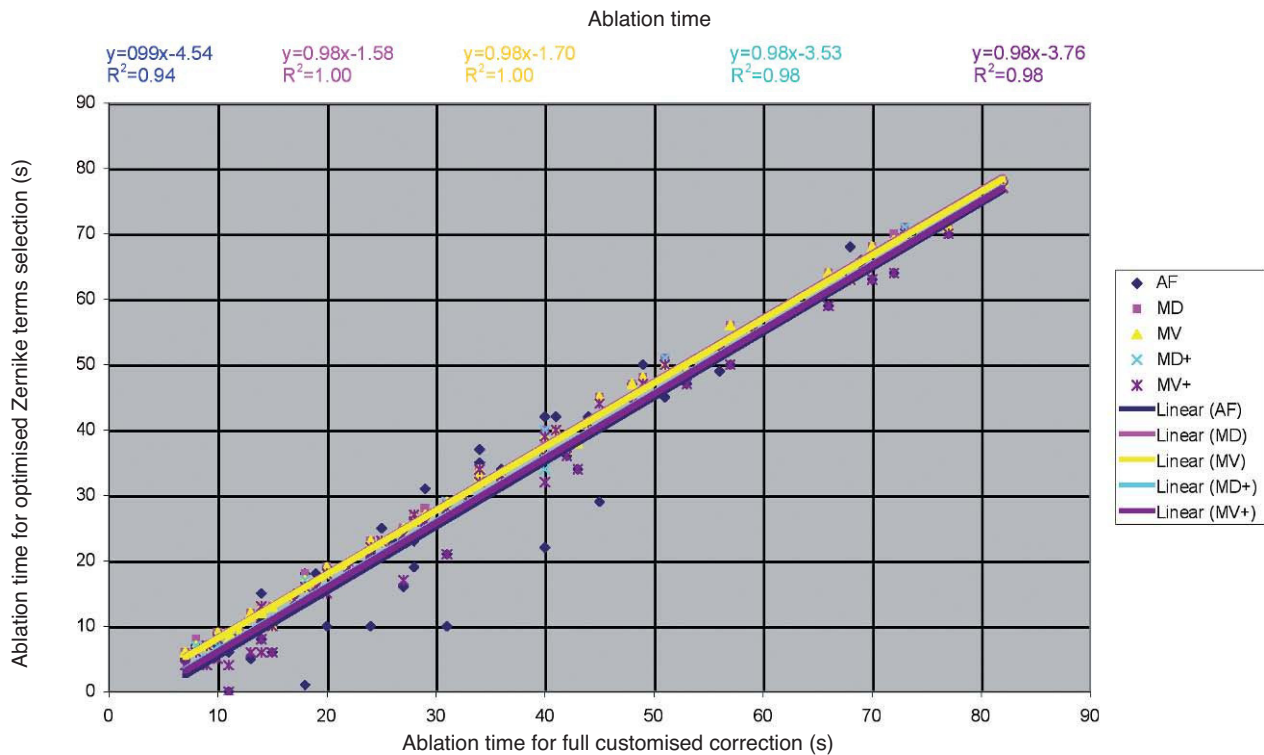


FIGURE 8

Ablation time for the “Optimal Zernike Term Selection” method (OZTS) vs. Ablation time for full customized correction, for the following modalities of OZTS: aberration-free correction (all HOA disabled) (AF, in blue), minimised depth (MD, in magenta), minimised volume (MV, in yellow), minimised depth+ (MD+, in cyan), and minimised volume+ (MV+, in purple).

a variation of the multizone concept. The problem comes, as well, from the aberrations that are induced (especially spherical aberration).

In the treatments designed having a smaller optical zone for the cylindrical component (or, in general, for the most powerful correction axis), the minimisation is based upon the concept of the maximal depth being based on the lowest meridional refraction and the selected optical zone, and the effective optical zone of the highest meridional refraction is reduced to match the same maximal depth. The problem comes again from the aberrations that are (especially high-order astigmatism).

In the boost-slider method, minimisation is achieved by means of a linear modulation of the ablated volume. The problem comes from the changes in refraction that are induced by the modulation.

In the Z-clip method, minimisation consists of defining a “saturation depth” for the ablated volume: in all those points where the ablation is designed to go deeper than the saturation value, the actual ablation depth is limited, being set to precisely that saturation value. The problem comes from the fact that this “saturation limit” may occur anywhere in the ablation area, compromising the refraction when those points are close to the ablation centre, and affecting the induction of aberrations in a complicated way.

In the Z-shift method, minimisation consists of defining a “threshold value” for the ablated volume, so that in those points where the ablated depth was designed to be less than that threshold value, no ablation is performed at all, and

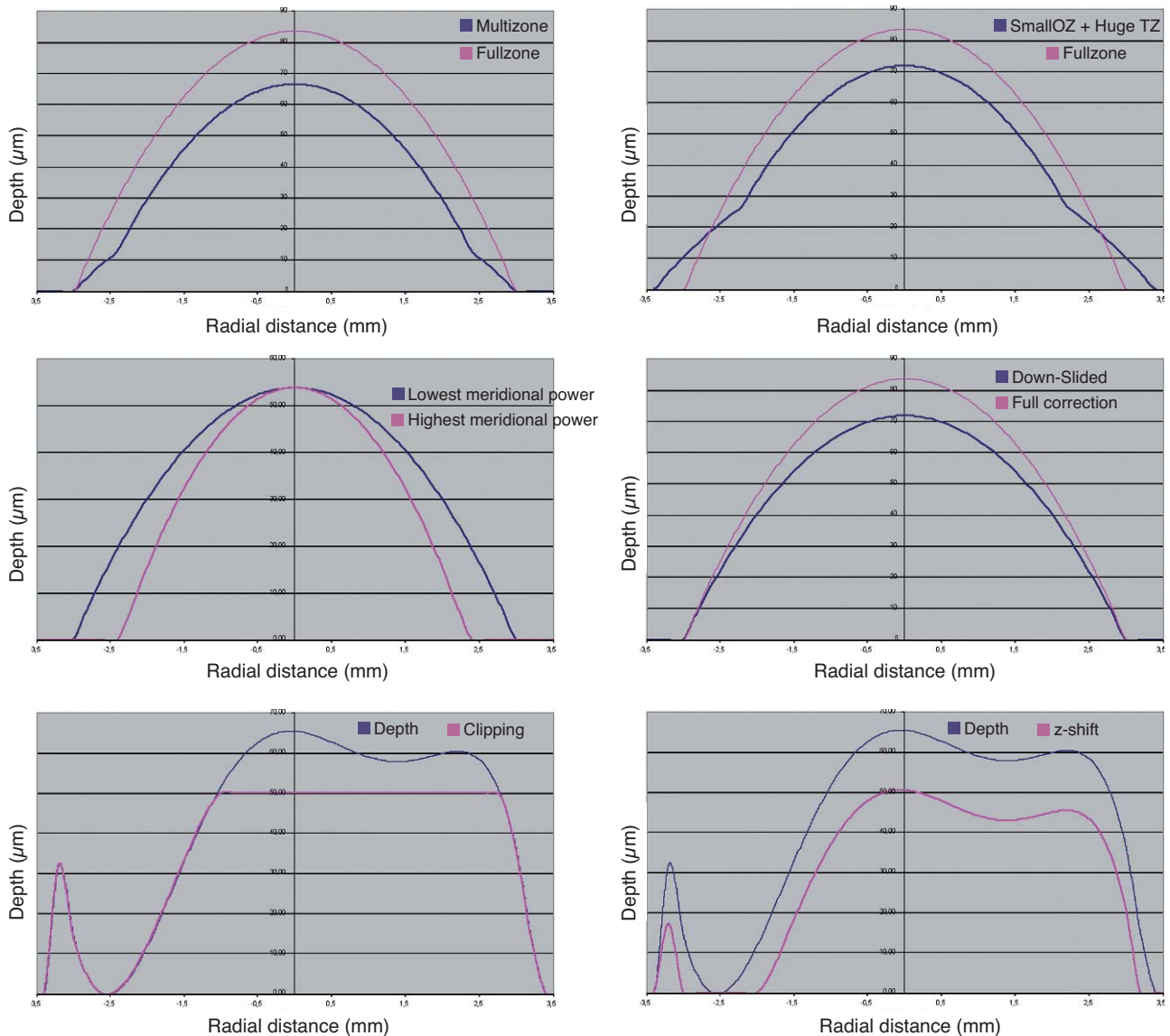
the rest of the points are ablated by an amount equal to the original planned ablation minus the threshold value. The problem comes from the fact that this “threshold value” may be reached anywhere in the ablation area, compromising the refraction when the below-threshold points are found close to the ablation centre, and the functional optical zone when they are found at the periphery.

Examples of each these methods can be found in *figure 9*.

The four minimisation approaches proposed in this work consists of simplifying the profile by selecting a subset of Zernike terms that minimises the necessary ablation depth or ablation volume while respecting the Zernike terms considered to be clinically relevant.

For each combination of Zernike terms, the low-order terms are recalculated using the Automatic Refraction Balance method described above, in such a way that the refractive correction is not compromised. Taking into account that the Zernike terms are either planned to be corrected or excluded, it does not compromise the visual performance because all those terms that are excluded (not planned to be corrected) are below clinical-relevance levels. The proposed approaches are safe, reliable and reproducible due to the objective foundation upon which they are based. In the same way, the selected optical zone will be used for the correction.

It is important to remark that the selection of the Zernike terms to be included in the correction is not trivial. Only those Zernike terms considered to be not clinically relevant or of minor clinical relevance can be excluded from the correction, but they don't have to be necessarily excluded. Actually,

**FIGURE 9**

Different methods for the minimisation of the amount of ablated tissue (blue line): by means of multizonal treatments, by means of a smaller optical zone treatments with a large transition zone, by means of a smaller optical zone for the astigmatic correction, by means of a boost slider (down-slided), by means of a Z-clip method, and by means of a Z-shift method. In all cases, the pink line indicates the required ablation profile to without minimization.

individual Zernike terms considered to be not clinically relevant will only be used (or not) when they entail an extra amount of tissue for the ablation, and they will be enabled (included) when they help to save tissue for the ablation.

In this way, particular cases are represented by the full wavefront correction, by disabling all non-clinically relevant terms, or by disabling all high-order terms.

The selection process is completely automatic and driven by a computer, ensuring systematic results and a minimisation of the amount of tissue to be ablated. This automation also simplifies the foreseeable problems of manually selecting the adequate set of terms.

A criticism to this methodology can be that fact that we are not targeting diffraction-limited optical system. That means we are reducing the ablated tissue at the cost of accepting a “trade-off” in the optical quality. However, it is still

not known precisely whether an “optically perfect eye” after surgery is better than preserving the aberrations that the eye had before surgery. Although the optical quality of the eye can be described in terms of the aberration of its wavefront, it was observed that those individuals with smaller aberration in their wavefront were not always those getting the best visual-quality scores. From that, the optical quality of the human eye does not determine in a one-to-one way its visual quality. The concept of neural compensation indicates that the visual quality we have is somewhat superior to the optical quality that our eye provides, because the visual system seems to be adapted to the eye’s own aberration pattern.

The optical quality in an individual can be maximized for a given wavelength by cancelling the aberration of his wavefront and optimizing his defocus (for a single distance), but this has direct and dramatically negative implications for

the optical quality for the rest of wavelengths (the greater the negative effect the more extreme is the wavelength).²⁵ However, the optical quality of a person showing a certain degree of aberration of his wavefront decreases, relative to the maximum obtainable quality in the absence of aberration, but it has direct positive implications in the "stability" of the optical quality for a wide range of wavelengths (which covers the spectral sensitivity of the human eye).

The implications of this concept is very interesting because, for example, a patient corrected for his wave aberration represents a case in which despite having been improved his (monochromatic) optical quality in focus, his (polychromatic) visual quality is reduced. This confirms that it is not always advantageous or advisable to correct for all aberrations of an individual aspiring to obtain a monochromatically diffraction-limited optical system, as the chromatic blur would compromise his visual quality. Another positive implication that the wave aberrations may have on the visual function is that although it produces an overall blur, the wave aberration also brings depth of focus, i.e., some stability in terms of visual quality for a range of distances that can be considered to be simultaneously "in-focus". Lastly, moderate levels of wave aberration favour the stability of the image quality for wide visual fields.²⁶

This way, there are at least three criteria (chromatic blur, depth of focus, wide-field vision) favouring the option of leaving minor amounts of non-clinically-relevant aberrations.

Besides, there are no foreseeable risks derived from the proposed minimisation functions because they propose ablation profiles that are simpler than the full-wavefront corrections.

However, some drawbacks and potential improvements may be hypothesised:

There may be a sort of "edge" problem, related to the fact that a Zernike term with DEq of 0.49 D may be enabled or disabled, due to its expected minor clinical relevance, whereas a Zernike term with DEq of 0.51 D needs to be corrected (according to our selection criteria).

It is controversial, as well, whether or not one can consider the clinical relevance of every Zernike term independently. The visual effect of an aberration does not only depend on it but also on the other aberrations that are present in the full pattern; for example, a sum of small, and previously considered clinically irrelevant aberrations, could involve a clear loss of overall optical quality.

A possible improvement comes from the fact that current selection strategy consists of a binary "ON/OFF" approach for each Zernike term. However, better corrections and higher amounts of tissue saving might be obtained by using a correcting factor $F[n,m]$ (range 0 to 1) for each Zernike correcting a wavefront of the form:

$$AbI(\rho, \theta) = \sum_{n=0}^{\infty} \sum_{m=-n}^{+n} F_n^m C_n^m Z_n^m(\rho, \vartheta) \quad (4)$$

However, this would come to a much higher computational cost.

Another possible improvement would be to consider possible aberration couplings, at least, between Zernike

modes of the same angular frequency as a new evaluation parameter.

In this work, as well, a method to objectively determine the actual clinical relevance of individual terms in a Zernike expansion of the wave aberration was described.

A method to objectively minimise the maximum depth or volume of a customised ablation based on the Zernike expansion of the wave aberration was provided in the present work.

Based upon a sample population of 100 wavefront maps, the tissues-saving capabilities of this method to minimise the amount of required ablated tissue were simulated.

The wavefront maps that were used were derived only from corneal aberrations (from which defocus, for example, cannot be determined). Moreover, correcting corneal aberrations does not imply eliminating the correspondent for the eye, as it depends also on internal aberrations. However, the proposed methods tries to minimize the amount of ablated tissue in a Zernike-based customized treatment irrespective of the origin of the wavefront map.

In summary, this study demonstrated that it is possible to develop new algorithms and ablation strategies to perform efficient laser corneal refractive surgery in a customized form, minimising the amount of ablated tissue without compromising the visual quality. The availability of such profiles, potentially maximising visual performance without increasing the risk factors, would be of great value for the refractive surgery community and, ultimately, for the patients' health and safety.

Further clinical evaluations on human eyes are needed to confirm the preliminary simulated results presented herein.

REFERENCES

- Munnerlyn CR, Koons SJ, Marshall J. Photorefractive keratectomy: a technique for laser refractive surgery. *J Cataract Refract Surg.* 1988; 14:46-52.
- Mastropasqua L, Toto L, Zuppari E, et al. Photorefractive keratectomy with aspheric profile of ablation versus conventional photorefractive keratectomy for myopia correction: six-month controlled clinical trial. *J Cataract Refract Surg.* 2006;32:109-116.
- Buratto L, Ferrari M, Rama P. Excimer laser intrastromal keratomileusis. *Am J Ophthalmol.* 1992;113:291-295.
- Pallikaris IG, Siganos DS. Excimer laser in situ keratomileusis and photorefractive keratectomy for correction of high myopia. *J Refract Corneal Surg.* 1994;10:498-510.
- Ditzen K, Huschka H, Pieger S. Laser in situ keratomileusis for hyperopia. *J Cataract Refract Surg.* 1998;24:42-47.
- el Danasoury MA, Waring GO 3rd, el Maghraby A, Mehrez K. Excimer laser in situ keratomileusis to correct compound myopic astigmatism. *J Refract Surg.* 1997;13:511-520.
- Moreno-Barriuso E, Lloves JM, Marcos S. Ocular Aberrations before and after myopic corneal refractive surgery: LASIK-induced changes measured with LASER ray tracing. *Invest Ophthalmol Vis Sci.* 2001; 42:1396-1403.
- Artal P. What aberration pattern (if any) produces the best vision?, 6th International Congress of Wavefront Sensing & Optimized Refractive Corrections, Athens, Greece; February 2005.
- Applegate RA, Howland HC. Refractive surgery, optical aberrations, and visual performance. *J Refract Surg.* 1997;13:295-299.
- Artal P, Chen L, Fernandez EJ, Singer B, Manzanera S, Williams DR. Neural compensation for the eye's optical aberrations. *J Vis.* 2004;4: 281-287.
- Thibos LN, Hong X, Bradley A, Applegate RA. Accuracy and precision of objective refraction from wavefront aberrations. *Journal of Vision.* 2004;4:329-351.
- Salmon TO. Corneal contribution to the wavefront aberration of the eye. PhD Dissertation. 1999:70.

13. Mrochen M, Jankov M, Bueeler M, Seiler T. Correlation Between Corneal and Total Wavefront Aberrations in Myopic Eyes. *J Refract Surg.* 2003;19:104-112.
14. Alio JL, Belda JI, Osman AA, Shalaby AM. Topography-guided laser in situ keratomileusis (TOPOLINK) to correct irregular astigmatism after previous refractive surgery. *J Refract Surg.* 2003;19:516-527.
15. Mrochen M, Kaemmerer M, Seiler T. Clinical results of wavefront-guided laser in situ keratomileusis 3 months after surgery. *J Cataract Refract Surg.* 2001;27:201-207.
16. Mrochen M, Donetzky C, Wüllner C, Löffler J. Wavefront-optimized ablation profiles: Theoretical background. *J Cataract Refract Surg.* 2004;30:775-785.
17. Koller T, Iseli HP, Hafezi F, Mrochen M, Seiler T. Q-factor customized ablation profile for the correction of myopic astigmatism. *J Cataract Refract Surg.* 2006;32:584-589.
18. Gatinel D, Malet J, Hoang-Xuan T, Azar DT. Analysis of customized corneal ablations: theoretical limitations of increasing negative asphericity. *Invest Ophthalmol Vis Sci.* 2002;43:941-948.
19. Mattioli R, Tripoli NK. Corneal Geometry Reconstruction with the Keratron Videokeratographer. *Optom Vis Sci.* 1997;74:881-894.
20. Zernike F. Diffraction theory of the knife-edge test and its improved form, the phase-contrast method. *Monthly Notices of the Royal Astronomical Society.* 1934;94:377-384.
21. Thibos LN, Applegate RA, Schwiegerling JT, Webb R, VSIA Standards Taskforce Members. Standards for Reporting the Optical Aberrations of Eyes. *J Refract Surg.* 2002;18:S652-S660.
22. Thibos LN. Wavefront Data Reporting and Terminology. Second International Wavefront Congress in Monterey, CA. 1999. Available at: <http://research.opt.indiana.edu/Library/WavefrontReporting/WavefrontReporting.html>. Accessed: 16 December 2008.
23. Thibos LN, Wheeler W, Horner D. A vector method for the analysis of astigmatic refractive errors. In: *Vision Science and Its Applications*, vol 2. 1994 OSA Technical Digest Series. Washington, DC: Optical Society of America, 1994:14-17.
24. Remón L, Tornel M, Furlan WD. Visual Acuity in Simple Myopic Astigmatism: Influence of Cylinder Axis. *Optom Vis Sci.* 2006;83:311-315.
25. McLellan JS, Marcos S, Prieto PM, Burns SA. Imperfect optics may be the eye's defence against chromatic blur. *Nature.* 2002;417:174-176.
26. Bará S, Navarro R. Wide-field compensation of monochromatic eye aberrations: expected performance and design trade-offs. *J Opt Soc Am A.* 2003;20:1-10.

APPENDIX 1
Objective Wavefront Refraction from Low-Order Zernike Modes

A common way to fit an arbitrarily aberrated wavefront with a quadratic surface is to find the surface that minimizes the sum of the squared deviations between the two surfaces. The least-square fitting method is the basis of the Zernike wavefront expansion. Since the Zernike expansion employs an orthogonal set of basic functions, the least-square solution is simply given by the second-order Zernike coefficients of the aberrated wavefront, regardless of the values of the other coefficients. These second-order Zernike coefficients can be converted into a spherocylindrical prescription in power-vector notation of the form $[J_0, M, J_{45}]$.

$$J_0 = \frac{-8\sqrt{6}C_2^{+2}}{PD^2} \tag{A1.1}$$

$$M = \frac{-16\sqrt{3}C_2^0}{PD^2} \tag{A1.2}$$

$$J_{45} = \frac{-8\sqrt{6}C_2^{-2}}{PD^2} \tag{A1.3}$$

Where PD is the pupil diameter, M is the spherical equivalent, J_0 , the cardinal astigmatism and J_{45} the oblique astigmatism. The components J_0 , M, and J_{45} represent the power of a Jackson crossed cylinder with axes at 0 and 90°, the spherical equivalent power, and the power of a Jackson crossed cylinder with axes at 45 and 135°, respectively.

The power-vector notation is a cross-cylinder convention that is easily transposed into conventional refractions in terms of sphere, cylinder, and axis in the minus-cylinder or plus-cylinder formats used by clinicians.

$$S = M - \frac{C}{2} \tag{A1.4}$$

$$C = 2\sqrt{J_0^2 + J_{45}^2} \tag{A1.5}$$

$$A = \frac{\arctan\left(\frac{J_{45}}{J_0}\right)}{2} \tag{A1.6}$$

The same low-order Zernike modes can be used to calculate the refraction for any given smaller pupil size, either by refitting the raw wave-aberration data to a smaller diameter, or by mathematically performing the so-called radius transformation of the Zernike expansion to a smaller diameter.

APPENDIX 2
Automatic Manifest Refraction Balance

The mathematical formulation is:

$$J_{0,MR} = \frac{-C_{MR}}{2} \cos(2A_{MR}) \tag{A2.1}$$

$$M_{MR} = S_{MR} + \frac{C_{MR}}{2} \tag{A2.2}$$

$$J_{45,MR} = \frac{-C_{MR}}{2} \sin(2A_{MR}) \tag{A2.3}$$

$$J_{0,MR} = J'_{0,LOA} + J_{0,LOA(PD) \rightarrow LOA(4mm)} \tag{A2.4}$$

$$M_{MR} = M'_{LOA} + M_{HOA(PD) \rightarrow LOA(4mm)} \tag{A2.5}$$

$$J_{45,MR} = J'_{45,LOA} + J_{45,HOA(PD) \rightarrow LOA(4mm)} \tag{A2.6}$$

$$C_2^{-2}(HOA(PD) \rightarrow LOA(4mm)) = f(C_n^{-2}(PD)) \tag{A2.7}$$

$$C_2^0(HOA(PD) \rightarrow LOA(4mm)) = f(C_n^0(PD)) \tag{A2.8}$$

$$C_2^{+2}(HOA(PD) \rightarrow LOA(4mm)) = f(C_n^{+2}(PD)) \quad (A2.9)$$

$$C_2^{-2}(PD) = \frac{-J'_{45,LOA} PD^2}{8\sqrt{6}} \quad (A2.10)$$

$$C_2^0(PD) = \frac{-M'_{LOA} PD^2}{16\sqrt{3}} \quad (A2.11)$$

$$C_2^{+2}(PD) = \frac{-J'_{0,LOA} PD^2}{8\sqrt{6}} \quad (A2.12)$$

APPENDIX 3

Calculation of the Ablation Depth

Wavefront correction can be achieved by applying the reverse wavefront. Because a refractive surgery laser system can remove tissue rather than add tissue, the wavefront correction must also be taken into consideration by shifting the ablation profile from negative values to only positive values. Furthermore, the correction will be performed by modifying the anterior front surface of the cornea by means of photoablation. Thus, the change in the refractive index of air (n=1) and the cornea (n=1.376) boundary must be included. Applying these considerations, one will get:

$$Abl(\rho, \theta) = \frac{WA(\rho, \theta) - \min[WA(\rho, \theta)]}{n_{Cornea} - n_{Air}} \quad (A3.1)$$

where Abl(ρ,θ) is the ablation at a given point (in polar coordinates), WA the wave aberration, and n_{cornea} and n_{air} the refractive indices of the cornea and the air respectively.

The rigorous formulation of these minimised-depth functions is to find a vector of values E[n,m] (1 for enable, 0 for disable) that minimises the maximum ablation depth, conditioned to enabling the terms that have an optical blur dioptric equivalent above 0.25 D or 0.50 D (in yellow or red), respectively.

$$Abl(\rho, \theta) = \quad (A3.2)$$

$$= \frac{\sum_{n=0}^{\infty} \sum_{m=-n}^{+n} E_n^m C_n^m Z_n^m(\rho, \theta) - \min \left[\sum_{n=0}^{\infty} \sum_{m=-n}^{+n} E_n^m C_n^m Z_n^m(\rho, \theta) \right]}{n_{Cornea} - n_{Air}}$$

This is equivalent to minimising the peak-to-valley value of the wavefront.

$$MaxAbl =$$

$$= \frac{\max \left[\sum_{n=0}^{\infty} \sum_{m=-n}^{+n} E_n^m C_n^m Z_n^m(\rho, \theta) \right] - \min \left[\sum_{n=0}^{\infty} \sum_{m=-n}^{+n} E_n^m C_n^m Z_n^m(\rho, \theta) \right]}{n_{Cornea} - n_{Air}} \quad (A3.3)$$

APPENDIX 4

Calculation of the Ablation Volume

The rigorous formulation of these minimised-volume functions is, again, to find a vector of values E[n,m] (1 for enable, 0 for disable) that minimises the total ablation volume, conditioned to enabling those terms whose optical blur dioptric equivalent is above 0.25 D or 0.50 D (in yellow or red) respectively.

$$AblVol = \int_0^{2\pi} \int_0^1 Abl(\rho, \theta) \rho d\rho d\theta \quad (A4.1)$$

$$= \int_0^{2\pi} \int_0^1 \frac{\sum_{n=0}^{\infty} \sum_{m=-n}^{+n} E_n^m C_n^m Z_n^m(\rho, \theta) - \min \left[\sum_{n=0}^{\infty} \sum_{m=-n}^{+n} E_n^m C_n^m Z_n^m(\rho, \theta) \right]}{n_{Cornea} - n_{Air}} \rho d\rho d\theta \quad (A4.2)$$

Taking into account that:

$$\int_0^{2\pi} \int_0^1 Z_n^m(\rho, \theta) \rho d\rho d\theta = 0 \quad (A4.3)$$

This leads to:

$$AblVol = \int_0^{2\pi} \int_0^1 \frac{-\min \left[\sum_{n=0}^{\infty} \sum_{m=-n}^{+n} E_n^m C_n^m Z_n^m(\rho, \theta) \right]}{n_{Cornea} - n_{Air}} \rho d\rho d\theta \quad (A4.4)$$

This is equivalent to maximising the minimum value of the wavefront.

$$AblVol = \pi \frac{OZ^2}{4} \frac{-\min \left[\sum_{n=0}^{\infty} \sum_{m=-n}^{+n} E_n^m C_n^m Z_n^m(\rho, \theta) \right]}{n_{Cornea} - n_{Air}} \quad (A4.5)$$